Variability and future decreases in winter wave heights in the Western North Pacific

Article *in* Geophysical Research Letters · March 2016

DOI: 10.1002/2016GL067924

3 authors:

Tomoya Shimura

Kyoto University

Nobuhito Mori

Kyoto University

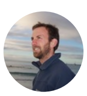

Mark A. Hemer

The Commonwealth Scientific and Industrial …

Geophysical Research Letters

RESEARCH LETTER
10.1002/2016GL067924

Key Points:
- Robust future decreases in winter wave heights over the Western North Pacific
- The West Pacific (WP) pattern-related wave climate change
- The effects of remotely generated swells on wave climate changes along a local coast

Supporting Information:
- Supporting Information S1

Correspondence to:
T. Shimura,
shimura@storm.dpri.kyoto-u.ac.jp

Citation:
Shimura, T., N. Mori, and M. A. Hemer (2016), Variability and future decreases in winter wave heights in the Western North Pacific, *Geophys. Res. Lett.*, *43*, doi:10.1002/2016GL067924.

Received 27 JAN 2016
Accepted 22 FEB 2016
Accepted article online 26 FEB 2016

Variability and future decreases in winter wave heights in the Western North Pacific

Tomoya Shimura[1], Nobuhito Mori[1], and Mark A. Hemer[2]

[1]Disaster Prevention Research Institute, Kyoto University, Kyoto, Japan, [2]Oceans and Atmosphere, Commonwealth Scientific and Industrial Research Organisation, Hobart, TAS, Australia

Abstract Ocean surface wave climate is a key consideration for a number of industrial and environmental systems, both offshore and at the coast. A dynamical spectral wave model forced with global climate models (GCMs) was used to produce an ensemble of simulations of both historical and projected future wave climate. To estimate the uncertainty of the projected wave climate, we combined a multimember ensemble experiment using MRI-AGCM3.2H with a multimodel ensemble using eight CMIP5 GCMs. Future changes in wintertime wave heights from the end of the 20th to the 21st century were analyzed. Projected decreases in wave heights over the Western North Pacific are highly consistent among the ensemble. The future decreases in wave heights are significantly related to changes in the West Pacific pattern. Both locally generated waves and remotely generated swells are important to estimate future changes in the wave climate on a regional scale.

1. Introduction

Long-term characteristics of ocean surface waves (wave climate) are a key consideration for coastal disaster management, beach morphology evolution, nearshore environment and marine renewable energy resource estimation. Assessing projected 21st century wave climate changes are thus relevant for future planning in these fields. Ocean wave climate changes under future climate scenarios have been projected for time scales of 20–100 years by several research groups [*Hemer et al.*, 2013; *Shimura et al.*, 2015]. Future mean significant wave heights are projected to differ from present climate values by up to ±10% by the end of the 21st century. Although changes to the mean wave climate are becoming clearer with recent efforts in wave climate projection, the uncertainty remains poorly resolved given the small amount of available wave climate projection data. Studies to date [*Hemer et al.*, 2013] suggest that the major sources of uncertainty in wave climate projections are emission scenarios, Global Climate Models (GCM), and downscaling and wave modeling approaches.

Climate projections are generally based on GCM climate simulations forced with future greenhouse gas emission/concentration scenarios. The (un)certainty and robustness of the projected climate is estimated on the basis of (in)consistency across an ensemble of model simulations. Large uncertainties are associated with wave climate projections, owing to the low level of agreement between models and the limited number of available projections [*Church et al.*, 2013]. A few features of projected change are presented with greater confidence. For example, future increases in wave heights over the Southern Ocean associated with enhanced wind speeds is expected [*Church et al.*, 2013]. *Wang et al.* [2014] conducted statistical global wave projections using 20 GCMs and showed wave height increases in the eastern tropical Pacific.

The global circulation has a number of preferred patterns of variability (large-scale circulation patterns; e.g., the El Niño–Southern Oscillation), and understanding the nature and changes of these patterns is central to understanding regional climate variability and change [*Trenberth et al.*, 2007]. Wave climate variability has been shown to respond to these large-scale circulation patterns [e.g., *Shimura et al.*, 2013; *Stopa and Cheung*, 2014]. It is important to understand the relationship between wave climate variability and change and large-scale circulation patterns to reduce uncertainties in wave climate projections.

Recent studies [*Barnard et al.*, 2015] have demonstrated the strong relationship between spatial patterns of coastal change and El Niño and Pacific North American indices across the Pacific Basin. In the Western North Pacific (WNP) the relationship between these indices and coastal change was found to be weak relative to that observed along other margins of the Pacific Basin. This suggests a local complexity which is poorly resolved by the broad scale approach applied in that study. As a consequence, we focus our study on the coherent features of wave climate variability and change over the Western North Pacific. We assess the relationship between future changes in wave climate with large-scale circulation patterns considering projections uncertainty and interpret the change from a climatological viewpoint. Finally, we discuss the contrasting relationship of locally and distally generated (swell) waves with large-scale circulation patterns, and focus on the implications for coastal areas of Japan as an example.

2. Methodology

We conducted ensemble experiments adopting two conceptual approaches to ensemble wave climate projection. (1) A single GCM ensemble experiment consisting of running a single GCM with several experimental configurations. (2) A multi-GCM ensemble experiment using multiple GCMs of the fifth phase of the Coupled Model Intercomparison Project (CMIP5) [*Taylor et al.*, 2012] for two emission scenarios. These two different approaches help us to understand uncertainties that stem from given future conditions and models.

2.1. Single-GCM Ensemble Experiment

Shimura et al. [2015] carried out future global wave climate projections using the spectral wave model WAVEWATCH III [*Tolman*, 2009] forced with marine surface winds taken from climate simulations produced by the high-resolution atmospheric GCM (MRI-AGCM3.2H). The spatial resolution of the MRI-AGCM3.2H is 60 km, and the wave simulation resolution is 1° over the global domain. The MRI-AGCM3.2H experiment consists of 12 members with four sea surface temperature (SST) conditions and three cumulus convection schemes, under the A1B scenario. The time frame 1979 to 2009 is used for the present wave climate and 2075 to 2099 for the future climate.

In this study, wave climate projections under Representative Concentration Pathway 8.5 scenario (RCP8.5) [*Collins et al.*, 2013] are added to those of *Shimura et al.* [2015]. Atmospheric climate simulations by MRI-AGCM3.2H with four future SST conditions under the RCP8.5 scenario [*Mizuta et al.*, 2014] were used. The wave climate was simulated with WAVEWATCH III [*Tolman*, 2014] forced with 6-hourly surface winds and monthly sea ice fields of MRI-AGCM3.2H. The spatial resolution is 60 km globally. This experiment is described in detail in Text S1 and Table S1 in the supporting information.

2.2. Multi-GCM Ensemble Experiment

Climate simulations from eight CMIP5 AOGCMs under RCP4.5 and RCP8.5 scenarios were selected for the wave climate projections, following *Hemer and Trenham* [2015]. Global wave climate projections were carried out using WAVEWATCH III [*Tolman*, 2009] forced with 3-hourly marine surface winds and monthly sea ice fields from CMIP5 AOGCMs. The spatial resolution is 1° globally. The time frame 1979 to 2005 is used for the present wave climate and 2081 to 2100 for the future climate. This experiment is described in detail in the Text S2 and Table S2.

2.3. Wave Climate Hindcast

Besides the future wave climate projection, a high-resolution wave climate hindcast was conducted to discuss wave climate features along the Japan coast, as described in section 3.3. This wave climate hindcast was based on the state-of-the-art global atmospheric reanalysis data set, JRA-55 [*Kobayashi et al.*, 2015]. The spatial resolution of JRA-55 is 60 km. The wave climate from 1979 to 2009 was calculated using WAVEWATCH III with JRA-55 forcing. Spatial resolutions are 30 min for the North Pacific domain and 6 min for the nested Japan shoreline domain. This hindcast is described in detail in Text S3. In addition, wave observations by buoys around Japan collected by the Japan Meteorological Agency from 1979 to 2006 (http://www.data.jma.go.jp/gmd/kaiyou/db/wave/obsdata/usweqm_old.html) were used in order to support the results of wave climate hindcast.

3. Changes in Wave Climate and a Large-Scale Atmospheric Circulation Pattern

Robust projected changes in wave climate are identified, and these changes are attributed to a large-scale circulation pattern. The mean significant wave height is used as a representative value of the wave climate, and the future change is defined as future minus present climate value. The analysis below focuses on winter (December–January–February, denotes DJF) because wave climate response to large-scale circulation pattern is the strongest in winter [*Shimura et al.*, 2013; *Barnard et al.*, 2015].

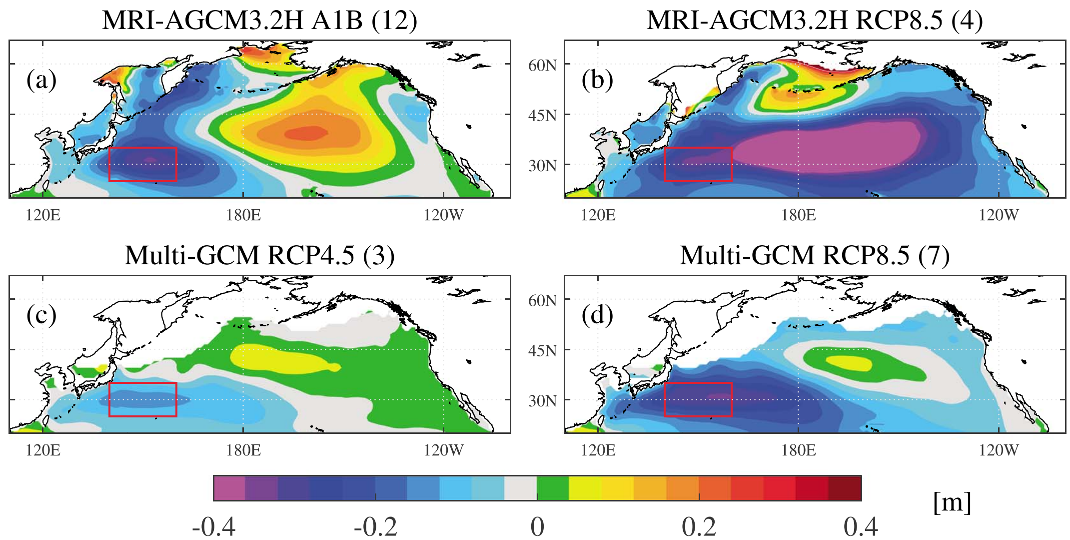

Figure 1. Future changes in wintertime mean wave heights: (a) Single-GCM ensemble experiment under A1B scenario (12 members), (b) Single-GCM ensemble experiment under RCP8.5 scenario (4 members), (c) Multi-GCM ensemble experiment under RCP4.5 scenario (8 members), (d) Multi-GCM ensemble experiment under RCP8.5 scenario (8 members). The number in parenthesis over each panel means the number of ensemble members showing statistically significant (tested by 5% significance level) decreases in wave heights in a red box.

3.1. Changes in Wave Heights Over the North Pacific

Figure 1 shows the future projected changes in wintertime mean wave heights for each ensemble experiment. All experiments show a decrease (up to −0.3 m) in the WNP at around 30°N (outlined with a red box in each panel). Although Figure 1 shows the ensemble mean, every ensemble member shows a projected decrease in this box, and in almost all cases (26/32 members) the decreases are significant, tested by *t* test at 5% significance level. Comparing across scenarios, the magnitude of the decrease is larger under a higher-rank scenario (RCP4.5 < A1B < RCP8.5). The projected decrease in winter wave heights in the WNP can be seen in previous studies [*Hemer et al.*, 2013] which were based on CMIP3 models. *Wang et al.* [2014] also showed decreases in wintertime wave heights in this region, using a statistical wave model and CMIP5 GCMs.

Given the results above, we conclude that the projected decrease in winter wave heights in the WNP are highly consistent among available future projections, and the projected changes have a higher level of confidence. In the Central and Eastern North Pacific Ocean, different experiments exhibit contrasting increasing or decreasing projected changes in wave height (different panels of Figure 1 show positive and negative changes for the same region), indicating a greater level of uncertainty in wave climate projections in these regions.

3.2. The Relationship Between Future Changes in Wave Climate and the West Pacific Circulation Pattern

Shimura et al. [2013] established a relationship between historical winter wave variability in the North Pacific and large-scale atmospheric circulation patterns. The West Pacific (WP) pattern dominates upper atmospheric variability over the North Pacific [*Wallace and Gutzler*, 1981] (see detail of WP pattern in Text S4). *Shimura et al.* [2013] found that a meridional shift of extratropical storm tracks corresponds to the WP pattern with a band-like shape of wave height variability in the North Pacific (see Text S5). Wave height variability around 30°N in the WNP is dominated by this band-like pattern of wave climate variability. Therefore, we focus on the WP pattern in our discussion below.

The WP pattern is generally defined by variability in the upper atmospheric geopotential height on a given pressure level (e.g., 500 hPa height). Changes in 500 hPa height under future global warming include atmospheric circulation and thermodynamic changes (temperature increases) [*Shepherd*, 2014]. Future 500 hPa height would increase globally with future increases in temperature [*Hu et al.*, 2001] (Figure S2). WP pattern index defined by 500 hPa height can include the thermodynamic change. The thermodynamic change does not directly contribute to wave climate change. Therefore, we redefine the WP pattern by sea level pressure (SLP) because of the lower sensitivity of SLP to thermodynamic change [*Shepherd*, 2014]. As a consequence, our WP pattern can more strongly signify atmospheric circulation change without the thermodynamic signal.

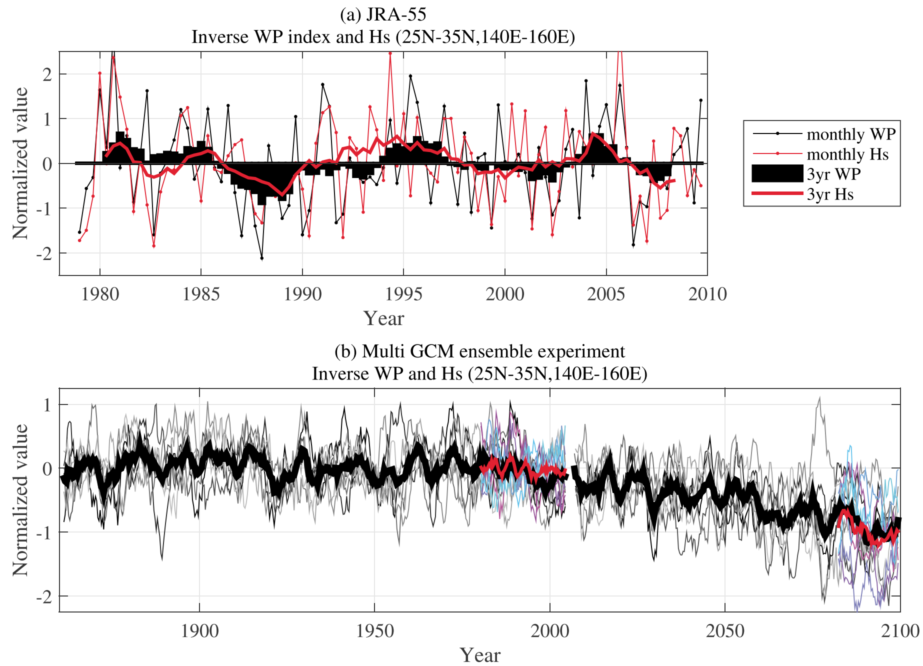

Figure 2. The WP index and winter mean wave heights around 30°N of the WNP (25°N–35°N and 140°E–160°E). (a) The values are derived from JRA-55. The values are the normalized and detrended monthly mean (thin lines) and the 3 year moving average (thick red line and black bar). (b) The values are derived from multi-GCM ensemble experiment under RCP8.5 scenario. The WP index is plotted in gray scale and the wave height is in color. Different model results are indicated with different shades of gray and color. Black and red thick lines are multimodel means for WP index and wave height. The values are 3 year moving averages normalized by present climate climatology (1860–2005 for WP index and 1979–2005 for wave height). "Normalized" indicates subtracting means and dividing by standard deviation for each calendar month. The inverse value of the WP index is plotted.

Over the middle to higher latitudes in the North Pacific, the SLP meridional gradient is larger (smaller) at the positive (negative) phases of the WP pattern. Thus, an SLP-based WP (SLP-WP) index is calculated as the averaged SLP difference between the middle latitude (140°E–160°W, 30°N–45°N) and the higher latitude (120°E–150°W, 45°N–70°N). The validity of SLP-WP index is described in Text S4. SLP-WP index is denoted as WP index hereafter.

Past and present climate relationships between wave height variability and the WP pattern are shown using the JRA-55. Figure 2a shows a time series of wave heights averaged over the WNP box (around 30°N) along with a time series of the inverse of the WP index. Note that this region of the WNP is the same region outlined in the red boxes plotted in Figure 1. The variability in wave height corresponds well to the WP index; the correlation coefficients are −0.56 and −0.74, significant at 5% significance level, for monthly and 3 year moving average values, respectively. Both the wave heights and the WP index clearly show the synchronized decadal oscillations (Figure 2a).

Figure 2b shows the time series of wintertime wave heights in the WNP and the WP index. Figure 2b displays the results for the multi-GCM ensemble experiment under an RCP8.5 scenario, but the other experiments show similar results. The wave climate simulation time periods are 1979–2005 for the present climate and 2081–2100 for the future climate, even though the SLP data from the CMIP5 GCMs are available over longer time frames. The WP index was calculated over the period 1860 to 2100 (CNRM-CM5 model is excluded for analysis due to data supply problem). The WP index shows no overall trend from 1860 to 2000; the WP index in the future climate, however, shows a clear positive trend (note that the inverse value for the WP index is plotted). Furthermore, wave heights decrease in the future climate by the same degree as the WP index change.

Figure 3 shows a correspondence between winter wave heights and the WP index. For the present climate (Figure 3a), the wave heights correlate negatively with the WP index, indicating that the models in this study can reproduce the relationship between wave height and WP index. Values averaged over the complete

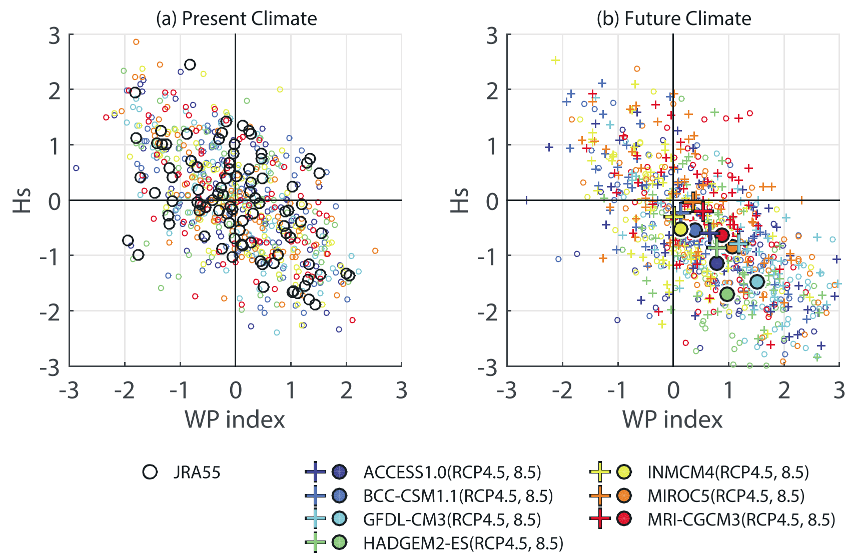

Figure 3. Correspondence of variability and future change between winter wave heights in the WNP and the WP index based on multi-GCM ensemble experiment. The color shading indicates the difference in models. (a) Normalized monthly mean value in the present climate with JRA-55 (black larger marker). (b) Normalized (by present climate value) monthly mean (smaller marker) and period mean values (larger marker) in the future climate. The cross markers indicate the values under RCP 4.5 and the circle markers indicate RCP 8.5 scenario.

future climate time frame (2081 – 2100) (larger markers in Figure 3b) shift to the lower right side in the future plot; this means that wave heights would decrease with a corresponding positive change in the WP index. The physics behind future changes in wave heights and the WP pattern is additionally discussed in Text S6.

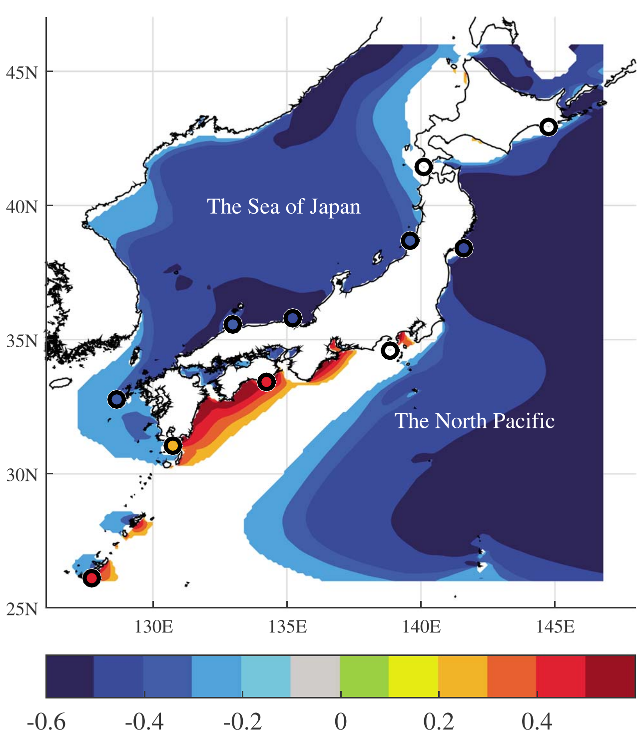

Figure 4. The correlation coefficient between winter monthly mean wave heights and the WP index based on JRA-55. The circle markers are for observations. Only regions with significant correlation at 5% significance level are colored.

3.3. Discussion: The WP Pattern-Related Wave Climate Change Along the Japan Coast

The large-scale mean wave climate of the WNP is clearly related to the WP index. We determine how the large-scale wave climate structure is altered at the more applied regional scale.

The higher-resolution historical wave climate "hindcast" around Japan is analyzed (see section 2.3). Figure 4 shows the correlation coefficient between winter monthly mean wave heights and the WP index based on a higher-resolution wave climate and buoy observations. The wave climate variability response along the Pacific coast of Japan shows variable relationships to the WP pattern; In the north, a negative correlation with the WP pattern is observed, whereas a positive correlation is observed along the south coast. In the Sea of Japan, a negative correlation is observed. The negative correlation is consistent with large-scale wave climate correlations in the WNP. An exception is the south Pacific coast of Japan where a positive change in the future WP

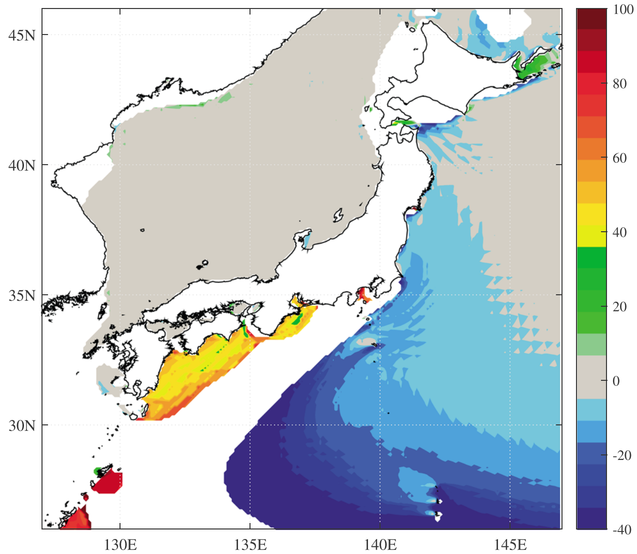

Figure 5. The estimated contributions of subtropics swells to the WP pattern-related wave climate variability around Japan (CWP_{sub}; definition is described in Text S7) (unit: %).

pattern would not lead to decrease in wave heights—contrary to the expected signal for wave heights over the WNP based on our analysis above.

This contrary relationship to the WP pattern is not seen in the sea surface wind speed variability, suggesting that it is a unique phenomenon of the local wave climate. One of the possible causes for the contrary response to the WP pattern can be attributed to remotely generated swells. During positive phases of the WP pattern, wave heights are larger with stronger winds over the subtropics, and vice versa (Text S5 and Figure S1). This is in contrast to the negative relationship between extratropical wave conditions and the WP pattern presented above. The effects of swells from subtropics are quantitatively analyzed by numerical experiments below. Figure 5 shows the estimated contributions of subtropics swells to the WP pattern-related wave climate variability around Japan (the method and data are described in Text S7 and Figures S5 and S6). Although the WP pattern-related wind waves gives significant impact on the wintertime mean wave climate over the WNP, the subtropics swell contributions are about 50% along the south coast of Japan. Therefore, the influence of the WP pattern on the local wave climate along the south coast results from mixed effects; there is a direct effect of local wind waves and a teleconnection effect of swells from the subtropics producing a positive correlation with WP index.

We have shown robust decreases in future winter wave heights over the WNP. However, the contribution analysis above leads us to speculate that future changes in wave climate along the south coast of Japan are uncertain [e.g., *Shimura et al.*, 2015, Figures 6a and 7a] because future projections of winds and related waves over the subtropics are not consistent across models [*Hemer et al.*, 2013].

While ocean surface waves are strongly forced by surface winds, winds and waves are generally not in equilibrium [*Fan et al.*, 2014], with the large component of wave power at a site being predominantly associated with swell waves propagated away from distant storms. Thus, while strong relationships between waves and large-scale circulation patterns can and have been identified [*Shimura et al.*, 2013], how these relate to observed waves at the coast can be complicated by the influence of swell which have conflicting relationships to the circulation pattern.

4. Conclusions

Ocean wave climates under a future global warming scenario were projected. This study estimated the robustness of wave climate projections using two types of ensemble experiments. The future greenhouse gas emission/concentration scenarios are given by A1B, RCP4.5, and RCP8.5 scenarios. It is found that projected decreases in winter wave heights over the WNP have higher degree of confidence because the projected future changes are highly consistent among the ensemble results. Furthermore, future decreases in wave heights correspond to positive changes in the WP pattern.

Although we showed robust decreases in future winter wave heights over the WNP, we noted that future changes along a local coast in the WNP, specifically the south coast of Japan, are uncertain. This is because the WP pattern-related wave climate variability along the south coast of Japan is different from that of the WNP, and the variability is significantly affected by remotely generated swells. In this study, which has focused on the Japanese coast, we have demonstrated the complexity of the wind wave/swell impacts on local wave climate variability and the implications of the complexities on projected local wave climate conditions. While *Fan et al.* [2014] explored the relative projected changes in both sea and swell components across the global ocean, our study has shown that focused—high-resolution—efforts are required to resolve regions of sea/swell dominance at scales more relevant to their application.

Several prior studies have projected wave climate exploiting statistical relationships between the atmospheric circulation and wave field [e.g., *Wang et al.*, 2014]. Our study indicates that projected wave conditions using these approaches—where the local wind sea will be well resolved, but swell less so—may exhibit greater certainty than it really has. Dynamical wave climate projection studies are able to provide estimates of the different components (although often overlooked), and increasingly statistical models are being developed, which provide consideration to distally generated swell [e.g., *Casas-Prat et al.*, 2014; *Perez et al.*, 2015]. We ask that future wave climate, associated impact, studies continue to give consideration to the complexities of wind waves/swell components of the wave field.

Acknowledgments
T.S. was supported by Japan Society for the Promotion of Science (JSPS) Fellowships for Young Scientists and Grant-in-Aid for JSPS Fellows (15J07767). This research was supported under the SOUSEI Program by the Ministry of Education, Culture, Sports, Science, and Technology (MEXT). The authors acknowledge the WCRP's Working Group on Coupled Modeling for the CMIP5 data sets (http://pcmdi9.llnl.gov/) and the Japan Meteorological Agency for JRA-55 data (http://jra.kishou.go.jp/JRA-55/index_en.html). Data set of wave climate projection of single-GCM ensemble experiment will be available by contacting T.S. (shimura@storm.dpri.kyoto-u.ac.jp). That of multi-GCM ensemble experiment will be available by contacting M.H. (mark.hemer@csiro.au).

References

Barnard, P. L., et al. (2015), Coastal vulnerability across the Pacific dominated by El Niño/Southern Oscillation, *Nat. Geosci.*, *8*(10), 801–807.

Casas-Prat, M., X. L. Wang, and J. P. Sierra (2014), A physical-based statistical method for modeling ocean wave heights, *Ocean Modell.*, *73*, 59–75.

Church, J., et al. (2013), Sea level change, in *Climate Change 2013: The Physical Science Basis. Contribution of Working Group I to the Fifth Assessment Report of the Intergovernmental Panel on Climate Change*, edited by T. F. Stocker et al., Cambridge Univ. Press, Cambridge, U. K., and New York.

Collins, M., et al. (2013), Long-term climate change: Projections, commitments and irreversibility, in *Climate Change 2013: The Physical Science Basis. Contribution of Working Group I to the Fifth Assessment Report of the Intergovernmental Panel on Climate Change*, edited by T. F. Stocker et al., Cambridge Univ. Press, Cambridge, U. K., and New York.

Fan, Y., S.-J. Lin, S. M. Griffies, and M. A. Hemer (2014), Simulated global swell and wind-sea climate and their responses to anthropogenic climate change at the end of the twenty-first century, *J. Clim.*, *27*(10), 3516–3536.

Hemer, M., Y. Fan, N. Mori, A. Semedo, and X. Wang (2013), Projected changes in wave climate from a multi-model ensemble, *Nat. Clim. Change*, *3*, 471–476.

Hemer, M. A., and C. E. Trenham (2015), Evaluation of a CMIP5 derived dynamical global wind wave climate model ensemble, *Ocean Modell.*, doi:10.1016/j.ocemod.2015.10.009.

Hu, Z.-Z., L. Bengtsson, E. Roeckner, M. Christoph, A. Bacher, and J. Oberhuber (2001), Impact of global warming on the interannual and interdecadal climate modes in a coupled GCM, *Clim. Dyn.*, *17*(5–6), 361–374.

Kobayashi, S., et al. (2015), The JRA-55 reanalysis: General specifications and basic characteristics, *Bull. Am. Meteorol. Soc.*, *93*(1), 5–48.

Mizuta, R., O. Arakawa, T. Ose, S. Kusunoki, H. Endo, and A. Kitoh (2014), Classification of CMIP5 future climate responses by the tropical sea surface temperature changes, *SOLA*, *10*, 167–171.

Perez, J., M. Menendez, P. Camus, F. J. Mendez, and I. J. Losada (2015), Statistical multi-model climate projections of surface ocean waves in Europe, *Ocean Modell.*, doi:10.1016/j.ocemod.2015.06.001.

Shepherd, T. G. (2014), Atmospheric circulation as a source of uncertainty in climate change projections, *Nat. Geosci.*, *7*, 703–708.

Shimura, T., N. Mori, and H. Mase (2013), Ocean waves and teleconnection patterns in the Northern Hemisphere, *J. Clim.*, *26*(21), 8654–8670.

Shimura, T., N. Mori, and H. Mase (2015), Future projection of ocean wave climate: Analysis of SST impacts on wave climate changes in the Western North Pacific, *J. Clim.*, *28*, 3171–3190.

Stopa, J. E., and K. F. Cheung (2014), Periodicity and patterns of ocean wind and wave climate, *J. Geophys. Res. Oceans*, *119*, 5563–5584, doi:10.1002/2013JC009729.

Taylor, K. E., R. J. Stouffer, and G. A. Meehl (2012), An overview of CMIP5 and the experiment design, *Bull. Am. Meteorol. Soc.y*, *93*(4), 485–498.

Tolman, H. (2009), User manual and system documentation of WAVEWATCH III^{TM} version 3.14, *Tech. Note 276, NOAA/NWS/NCEP/MMAB*, Maryland.

Tolman, H. (2014), User manual and system documentation of WAVEWATCH III version 4.18, *Tech. Note 316, NOAA/NWS/NCEP/MMAB*, Maryland.

Trenberth, K., et al. (2007), Observations: Surface and atmospheric climate change, in *Climate Change 2007: The Physical Science Basis. Contribution of Working Group I to the Fourth Assessment Report of the Intergovernmental Panel on Climate Change*, edited by S. Solomon, Cambridge Univ. Press, Cambridge, U. K., and New York.

Wallace, J. M., and D. S. Gutzler (1981), Teleconnections in the geopotential height field during the Northern Hemisphere winter, *Mon. Weather Rev.*, *109*(4), 784–812.

Wang, X., Y. Feng, and V. Swail (2014), Changes in global ocean wave heights as projected using multimodel CMIP5 simulations, *Geophys. Res. Lett.*, *41*, 1026–1034, doi:10.1002/2013GL058650.